Chapter 4

Absolute stability of systems with butterfly and multi-loop hysteresis

Nothing in life is to be feared, it is only to be understood. Now is the time to understand more, so that we may fear less.

—Marie Curie

We study the asymptotic stability of Lur'e systems with butterfly and multi-loop hysteresis nonlinearities modeled by the Preisach hysteresis operators with respect to a set of equilibrium points. We follow a differential approach as in [38] where a time-varying relation between the input and output rates of a given Preisach hysteresis operator that satisfies a sector boundary condition (under mild assumptions over the weighting function of the Preisach hysteresis operator) is established. In this way, we can analyze the interconnection as a Lur'e type system so that the classical circle criterion can directly be applied.

4.1 Input-output rate property of the Preisach butterfly hysteresis

We present in this section a differential formulation of the Preisach hysteresis operator that allows us to express explicitly the time-varying relation between the output rate and the input rate. When we consider an infinitesimal change to the input, the infinitesimal change to the output will be proportional to the infinitesimal state change of the hysterons that are located on the interface L_t and modulated by the associated weight. In other words, in our differential formulation of the Preisach hysteresis operator, we show that the output rate is proportional to input rate where the proportionality factor is given by a weighted line integral over the last horizontal or vertical linear segment of the interface L_t, corresponding to the instantaneous change of the relays' state on L_t. To properly state this, let us denote by L_t^+ and L_t^- the last horizontal and vertical linear segments of the

interface L_t respectively, defined by

$$L_t^+ = \{(\alpha,\beta) \in L_t \,|\, \alpha = u(t)\},$$
$$L_t^- = \{(\alpha,\beta) \in L_t \,|\, \beta = u(t)\}.$$

Then we define two functions $m_t : \mathscr{I} \to \mathbb{R}$ and $M_t : \mathscr{I} \to \mathbb{R}$, which will be used later in our main results, by

$$m_t = \inf_{\beta}\{\beta \,|\, (\alpha,\beta) \in L_t^+\},$$

$$M_t = \sup_{\alpha}\{\alpha \,|\, (\alpha,\beta) \in L_t^-\},$$

where we remove the dependence on L_t in the above notations for conciseness.

A simple interpretation of the scalar value of m_t and M_t can be made using the Preisach hysteresis operator memory behavior as studied in [11, 42]. In these books, the corners of L_t are given by the points in (α,β)-coordinates determined by the subset of extrema of the truncated input $u_t = \{u(\tau) \,|\, 0 \le \tau \le t\}$. In this regard, M_t and m_t correspond to the last maximum and last minimum of the truncated input u_t that are stored in the Preisach memory and coincide with the corner whose coordinates are given by $(\alpha,\beta) = \big[M_t, m_t\big]$.

Proposition 4.1. *Consider a Preisach hysteresis operator $\mathscr{P}$ as in* (2.3)*. Assume that $\dot{u} \in C(I,\mathbb{R})$ for some nonempty open interval $I \subset \mathbb{R}_+$. Then the time derivative of the Preisach hysteresis operator output $y \in AC(\mathbb{R}_+,\mathbb{R})$ at every time instant $t \in I$ is given by*

$$\dot{y}(t) = \psi(t)\dot{u}(t) \tag{4.1}$$

with

$$\psi(t) := \begin{cases} 2\displaystyle\int_{m_t}^{u(t)} \mu(u(t),\beta)\mathrm{d}\beta & \text{if } \dot{u}(t) > 0, \\ 2\displaystyle\int_{u(t)}^{M_t} \mu(\alpha,u(t))\mathrm{d}\alpha & \text{if } \dot{u}(t) < 0, \\ 0 & \text{otherwise.} \end{cases} \tag{4.2}$$

Proof. Let us first prove the case when $\dot{u}(t) > 0$ at some time instant $t \in I$. Since $\dot{u} \in C(I,\mathbb{R})$, there exists a constant $\Delta t > 0$ such that $\dot{u}(\tau) > 0$ for all $\tau \in [t, t+\Delta t]$. Assume without loss of generality that Δt is small enough to guarantee that $m_t = m_\tau$ for all $\tau \in$

$[t, t+\Delta t]$. Let us define three subsets of the Preisach domain given by

$$\begin{aligned}
\Omega_1 &:= \{(\alpha,\beta) \mid \alpha \geq \beta,\ u(t) \leq \alpha < u(t+\Delta t), \\
&\qquad\qquad u(t) \leq \beta < u(t+\Delta t)\} \\
\Omega_2 &:= \{(\alpha,\beta) \mid u(t) \leq \alpha < u(t+\Delta t),\ m_t \leq \beta < u(t)\} \\
\Omega_3 &:= \{(\alpha,\beta) \mid \alpha \geq \beta,\ m_t \leq \alpha < u(t),\ m_t \leq \beta < u(t)\},
\end{aligned}$$

and use them to partition P (see an illustration of such partition in Figure 4.1) such that the Preisach hysteresis operator output at t is given by

$$\begin{aligned}
y(t) = &- \iint\limits_{(\alpha,\beta)\in\Omega_1} \mu(\alpha,\beta)\,\mathrm{d}\alpha\mathrm{d}\beta - \iint\limits_{(\alpha,\beta)\in\Omega_2} \mu(\alpha,\beta)\,\mathrm{d}\alpha\mathrm{d}\beta \\
&+ \iint\limits_{(\alpha,\beta)\in\Omega_3} \mu(\alpha,\beta)\,\mathrm{d}\alpha\mathrm{d}\beta \\
&+ \iint\limits_{\substack{(\alpha,\beta)\in \\ P/(\Omega_1\cup\Omega_2\cup\Omega_3)}} \mu(\alpha,\beta)\,\left[\mathscr{R}^{\circlearrowleft}_{\alpha,\beta}\left(u, r_{\alpha,\beta}(L_0)\right)\right](t)\,\mathrm{d}\alpha\mathrm{d}\beta.
\end{aligned}$$

Since the relays $R^{\circlearrowleft}_{\alpha,\beta}$ with $(\alpha,\beta) \in P/(\Omega_1\cup\Omega_2\cup\Omega_3)$ have a constant output in the time interval $[t, t+\Delta t]$, the Preisach hysteresis operator output at a time instance $t+\Delta t$ is given by

$$\begin{aligned}
y(t+\Delta t) = &\\
&\iint\limits_{(\alpha,\beta)\in\Omega_1} \mu(\alpha,\beta)\,\mathrm{d}\alpha\mathrm{d}\beta + \iint\limits_{(\alpha,\beta)\in\Omega_2} \mu(\alpha,\beta)\,\mathrm{d}\alpha\mathrm{d}\beta \\
&+ \iint\limits_{(\alpha,\beta)\in\Omega_3} \mu(\alpha,\beta)\,\mathrm{d}\alpha\mathrm{d}\beta \\
&+ \iint\limits_{\substack{(\alpha,\beta)\in \\ P/(\Omega_1\cup\Omega_2\cup\Omega_3)}} \mu(\alpha,\beta)\,\left[\mathscr{R}^{\circlearrowleft}_{\alpha,\beta}\left(u, r_{\alpha,\beta}(L_0)\right)\right](t)\,\mathrm{d}\alpha\mathrm{d}\beta.
\end{aligned}$$

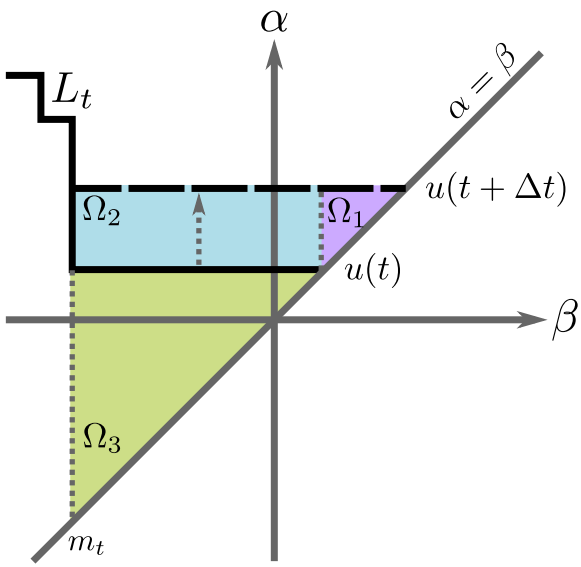

Figure 4.1: An illustration of a partitioning of the Preisach plane P that is used in the first part of the proof of Proposition 3.1. The domains Ω_1 (in purple), Ω_2 (in blue), and Ω_3 (in green) are defined according to the changes of the hysterons due to an increasing input (i.e., $\dot{u}(t) > 0$) in an infinitesimal time interval $[t, t+\Delta t]$.

Therefore the rate of change of the output can be computed by

$$\begin{aligned}
\frac{y(t+\Delta t)-y(t)}{\Delta t} &= \frac{y(t+\Delta t)-y(t)}{u(t+\Delta t)-u(t)} \frac{u(t+\Delta t)-u(t)}{\Delta t} \\
&= 2\left[\frac{\iint\limits_{(\alpha,\beta)\in\Omega_1} \mu(\alpha,\beta)\,\mathrm{d}\alpha\mathrm{d}\beta}{u(t+\Delta t)-u(t)} + \frac{\iint\limits_{(\alpha,\beta)\in\Omega_2} \mu(\alpha,\beta)\,\mathrm{d}\alpha\mathrm{d}\beta}{u(t+\Delta t)-u(t)} \right] \frac{\Delta u}{\Delta t} \\
&= 2\left[\frac{\int_{u(t)}^{u(t+\Delta t)} \int_{u(t)}^{\beta} \mu(\alpha,\beta)\,\mathrm{d}\alpha\mathrm{d}\beta}{u(t+\Delta t)-u(t)} + \frac{\int_{m_t}^{u(t)} \int_{u(t)}^{u(t+\Delta t)} \mu(\alpha,\beta)\,\mathrm{d}\alpha\mathrm{d}\beta}{u(t+\Delta t)-u(t)} \right] \frac{\Delta u}{\Delta t}.
\end{aligned}$$

By taking the limit $\Delta t \to 0$,

$$\dot{y}(t) = \left(2 \int_{m_t}^{u(t)} \mu(u(t), \beta) \, \mathrm{d}\beta \right) \dot{u}(t)$$

holds when $\dot{u}(t) > 0$. Consider now the case when $\dot{u}(t) < 0$ for some time instance $t \in I$. By similar arguments we can take $\Delta t > 0$ such that $\dot{u}(\tau) < 0$ for all $\tau \in [t, t+\Delta t]$ and assume without loss of generality that Δt is small enough to guarantee that $M_t = M_\tau$ for all $\tau \in [t, t+\Delta t]$. As before, let us define three subsets of the Preisach domain as follows

$$\begin{aligned}
\Omega_4 &:= \{(\alpha,\beta) \mid \alpha \geq \beta,\ u(t+\Delta t) \leq \alpha < u(t), \\
&\qquad\qquad u(t+\Delta t) \leq \beta < u(t)\} \\
\Omega_5 &:= \{(\alpha,\beta) \mid u(t) \leq \alpha < M_t,\ u(t+\Delta t) \leq \beta < u(t)\} \\
\Omega_6 &:= \{(\alpha,\beta) \mid a \geq b,\ u(t) \leq \alpha < M_t,\ u(t) \leq \beta < M_t\},
\end{aligned}$$

so that the Preisach plane P can be partitioned as illustrated in Figure 4.2. Accordingly, we can compute the rate of change of the output as follows

$$\begin{aligned}
\frac{y(t+\Delta t) - y(t)}{\Delta t} &= \frac{y(t+\Delta t) - y(t)}{u(t+\Delta t) - u(t)} \frac{u(t+\Delta t) - u(t)}{\Delta t} \\
&= -2 \left[\frac{\displaystyle\iint_{(\alpha,\beta)\in\Omega_4} \mu(\alpha,\beta) \, \mathrm{d}\alpha \mathrm{d}\beta}{u(t+\Delta t) - u(t)} + \frac{\displaystyle\iint_{(\alpha,\beta)\in\Omega_5} \mu(\alpha,\beta) \, \mathrm{d}\alpha \mathrm{d}\beta}{u(t+\Delta t) - u(t)} \right] \frac{\Delta u}{\Delta t} \\
&= -2 \left[\frac{\displaystyle\int_{u(t+\Delta t)}^{u(t)} \int_{\beta}^{u(t)} \mu(\alpha,\beta) \, \mathrm{d}\alpha \mathrm{d}\beta}{u(t+\Delta t) - u(t)} + \frac{\displaystyle\int_{u(t+\Delta t)}^{u(t)} \int_{u(t)}^{M_t} \mu(\alpha,\beta) \, \mathrm{d}\alpha \mathrm{d}\beta}{u(t+\Delta t) - u(t)} \right] \frac{\Delta u}{\Delta t}.
\end{aligned}$$

By taking the limit $\Delta t \to 0$, we obtain

$$\dot{y}(t) = \left(2 \int_{u(t)}^{M_t} \mu(\alpha, u(t)) \, \mathrm{d}\alpha \right) \dot{u}(t),$$

which holds for the case when $\dot{u}(t) < 0$. Finally, when $\dot{u}(t) = 0$ we have $\dot{y}(t) = 0$ and

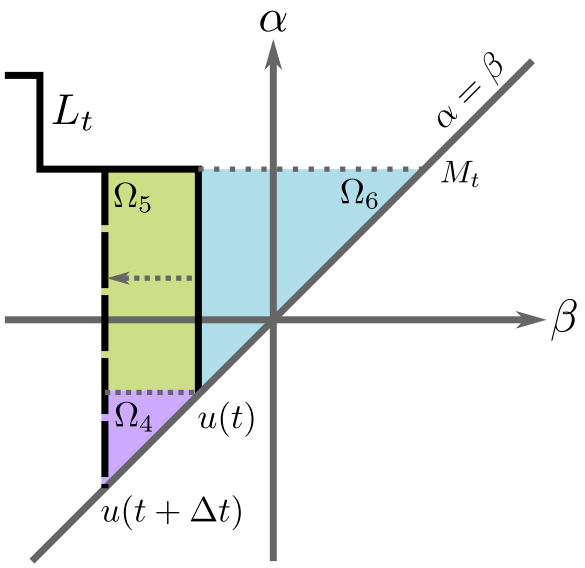

Figure 4.2: An illustration of a partitioning of the Preisach plane P that is used in the second part of the proof of Proposition 3.1. The domains Ω_4 (in purple), Ω_5 (in green), and Ω_6 (in blue) are defined according to the changes of the hysterons due to a decreasing input (i.e., $\dot{u}(t) < 0$) in an infinitesimal time interval $[t, t+\Delta t]$.

(4.1) holds. □

An immediate consequence of Proposition 4.1 is that when μ has a compact support, it is possible to find a sector bound for (4.2) which can be useful for the feedback loop analysis. We formalize this in the following proposition.

Proposition 4.2. *Suppose that $\mu \in C_{pw}(P,\mathbb{R})$ has a compact support. Then there exist $\lambda_m, \lambda_M \in \mathbb{R}$ with $\lambda_m \leq \lambda_M$ such that*

$$\lambda_m \leq \psi(t) \leq \lambda_M. \tag{4.3}$$

Proof. Let $P_1 \subset P$ be the compact support of μ. Then λ_m and λ_M are the extrema of (4.2) on P_1. In other words,

$$\lambda_m = 2 \min \left\{ \inf_{(\gamma,\kappa)\in P_1} \int_{\kappa}^{\gamma} \mu(\gamma,\beta)\mathrm{d}\beta, \inf_{(\gamma,\kappa)\in P_1} \int_{\kappa}^{\gamma} \mu(\alpha,\kappa)\mathrm{d}\alpha \right\} \tag{4.4}$$

and

$$\lambda_M = 2 \max \left\{ \sup_{(\gamma,\kappa)\in P_1} \int_{\kappa}^{\gamma} \mu(\gamma,\beta)\mathrm{d}\beta, \sup_{(\gamma,\kappa)\in P_1} \int_{\kappa}^{\gamma} \mu(\alpha,\kappa)\mathrm{d}\alpha \right\}. \tag{4.5}$$

□

In practice, when the Preisach hysteresis operator is used to model a physical phenomenon, it is commonly assumed that μ has a compact support which is partly due to the limited range of measurement data. We refer, for instance, to the works in [69,77,79]. We remark that a weaker condition on μ such that ψ lies in a sector bound is by requiring that the zero upper and lower partial moments of μ with respect to each of its arguments are finite.

Note that both Propositions 4.1 and 4.2 are valid for any Preisach hysteresis operator (2.3) regardless whether it has a sign-definite or sign-indefinite weighting function. In particular, it follows from Proposition 4.2 that when μ is positive semi-definite (resp., negative semi-definite) then $0 \leq \lambda_m \leq \lambda_M$ (resp. $\lambda_m \leq \lambda_M \leq 0$). On the other hand, when μ is sign-indefinite as in the case of the Preisach butterfly operator or a Preisach multi-loop operator, the sector bound of $\psi(t)$ satisfies $\lambda_m < 0 < \lambda_M$.

4.2 Set stability with Preisach butterfly hysteresis in the feedback loop

Let us now analyze the interconnection of a linear system with a Preisach butterfly operator in the feedback loop. We will focus on the set stability and convergence analysis. Consider the following feedback interconnection of linear system Σ_1 and a nonlinear operator Σ_2 as follows

$$\begin{aligned} \Sigma_1 : & \begin{aligned} \dot{x}(t) &= Ax(t) + Bv(t), \qquad x(0) = x_0, \\ z(t) &= Cx(t) \end{aligned} \\ \Sigma_2 : & y(t) = \big[\mathscr{P}(u, L_0)\big](t), \qquad L_0 \in \mathscr{I}, \\ & \qquad\qquad\qquad \text{with } v(t) = -y(t),\ u(t) = z(t), \end{aligned} \tag{4.6}$$

where $x(t) \in \mathbb{R}^n, z(t), v(t), y(t) \in \mathbb{R}$ and A, B, C are system matrices with suitable dimension and transfer function of Σ_1 is given by $G(s) = C(sI - A)^{-1}B$. The set of equilibria of the combined state of systems in the interconnection (4.6) is given by

$$\mathscr{E} = \{(x_{\rm ss}, L_{\rm ss}) \in \mathbb{R}^n \times \mathscr{I} \mid Ax_{ss} - B\mathscr{P}(Cx_{\rm ss}, L_{\rm ss}) = 0\}.$$

Proposition 4.3. *Let $\mathscr{P}$ be the Preisach hysteresis operator* (2.3) *with a compactly supported μ. Assume that (A, C) is observable and (A, B) is controllable. Suppose that $\overline{G}(j\omega)$ given by*

$$\overline{G}(j\omega) := (1 + \lambda_M G(j\omega))\,(1 + \lambda_m G(j\omega))^{-1}, \tag{4.7}$$

with λ_M and λ_m be as in (4.5) *and* (4.4) *is strictly positive real. Then $(x(t), L_t) \to \mathscr{E}$ as $t \to \infty$. Moreover, if A is invertible then*

$$\frac{\big[\mathscr{P}(z, L_0)\big](t)}{z(t)} \to \frac{1}{CA^{-1}B} \qquad \text{as } t \to \infty. \tag{4.8}$$

Proof. Using the differential form of $\mathscr{P}$ as given in (4.1) in Proposition 4.1, the output of the Preisach hysteresis operator $\mathscr{P}$ at any given time t can be expressed as

$$\begin{aligned} y(t) &= y(0) + \int_0^t \psi(\tau)\dot{u}(\tau)d\tau \\ &= \big[\mathscr{P}(u, L_0)\big](0) + \int_0^t \psi(\tau)\dot{u}(\tau)d\tau, \end{aligned} \tag{4.9}$$

where $\psi(t) \in [\lambda_m,\ \lambda_M]$ is as in (4.2). Using (4.9), an equivalent representation to (4.6) is given by the following piecewise time differentiable state equations

$$\begin{aligned} \ddot{x}(t) &= A\dot{x}(t) + B\dot{v}(t) \\ \dot{z}(t) &= C\dot{x}(t) \\ \dot{v}(t) &= -\psi(t)\dot{z}(t), \qquad \text{a.a. } t \in \mathbb{R}_+. \end{aligned} \tag{4.10}$$

This is illustrated in Figure 4.3. Consequently, by the circle criterion results [27, 31], the above interconnected system with time-varying sector-bounded ψ satisfying (4.7) is absolutely stable and $\dot{x}(t) \to 0$ as $t \to \infty$. It follows immediately from (4.6) that

$$Ax(t) - B\big[\mathscr{P}(z, L_0)\big](t) \to 0 \quad \text{as } t \to \infty,$$

and therefore the combined state $(x(t), L_t)$ of the closed-loop system approaches $\mathscr{E}$ as $t \to \infty$. Furthermore, when A is invertible, a simple algebraic computation to the above limit shows that (4.8) holds. □

From Proposition 4.3 we can see that the value of the ratio between the input and output of the Preisach hysteresis operator converges to the negative inverse of the zero frequency gain of the linear system. This means that the input-output phase plot of the Preisach hysteresis operator will approach a line crossing the origin with slope given by (4.8). We note that the conditions of observability, controllability and strict positive realness of $\overline{G}$ can be relaxed to stabilizability, detectability and positive realness conditions when the version of the circle criterion in [27, Corollary 9] is considered.

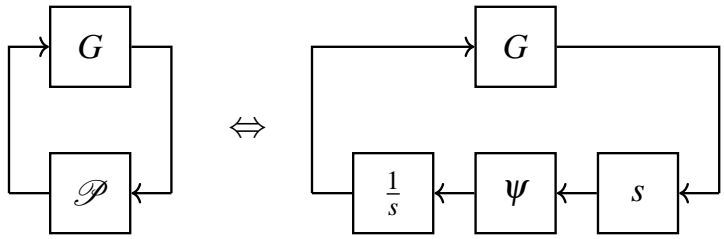

(a) (b)

Figure 4.3: Feedback equivalence of a linear system with Preisach hysteresis in the feedback loop: (a). The original feedback loop as in (4.6); (b). The equivalent loop as in (4.10) which is based on the differential formulation as in (4.1).

4.2.1 Numerical example: Lur'e system with butterfly hysteresis operator

Let us consider a numerical example to illustrate the results of the previous sections. Consider a feedback interconnection as in (4.6) with

$$A = \begin{bmatrix} 0 & 1 & 0 \\ 0 & 0 & 1 \\ -24 & -20 & -7 \end{bmatrix}, \quad B = \begin{bmatrix} 0 \\ 0 \\ 12 \end{bmatrix}, \quad C = \begin{bmatrix} 1 & 0 & 0 \end{bmatrix},$$

and the weighting function μ of $\mathscr{P}$ be defined by (3.4) in the example of Subsection 3.1.1. It is clear that P_1 is the compact support of μ and it can be checked that the sector bound defined in (4.4) and (4.5) satisfies $\lambda_m = -2$, $\lambda_M = 2$ and $\overline{G}_b(j\omega)$ defined as in (4.7) is strictly positive real. Therefore, following the result in Proposition 4.3, this feedback interconnection is stable and the steady state gain of the Preisach hysteresis operator converges to $\frac{1}{CA^{-1}B} = -2$. Fig. 4.4 shows the simulation results of this feedback interconnection with the initial states of the linear system given by $x_0 = [-0.7, -0.8, 0.9]^\top$, and the initial interface given by $L_0 = \{(\alpha, \beta) \in P \mid \beta = -0.7,\ \alpha \geq \beta\}$.

4.2.2 Numerical example: Lur'e system with multi-loop hysteresis operator

Consider a feedback interconnection as in (4.6) whose linear system matrices are given by

$$A = \begin{bmatrix} 0 & 1 & 0 \\ 0 & 0 & 1 \\ -26 & -28 & -3 \end{bmatrix}, \quad B = \begin{bmatrix} 0 \\ 0 \\ -26 \end{bmatrix}, \quad C = \begin{bmatrix} 1 & 0 & 0 \end{bmatrix}.$$

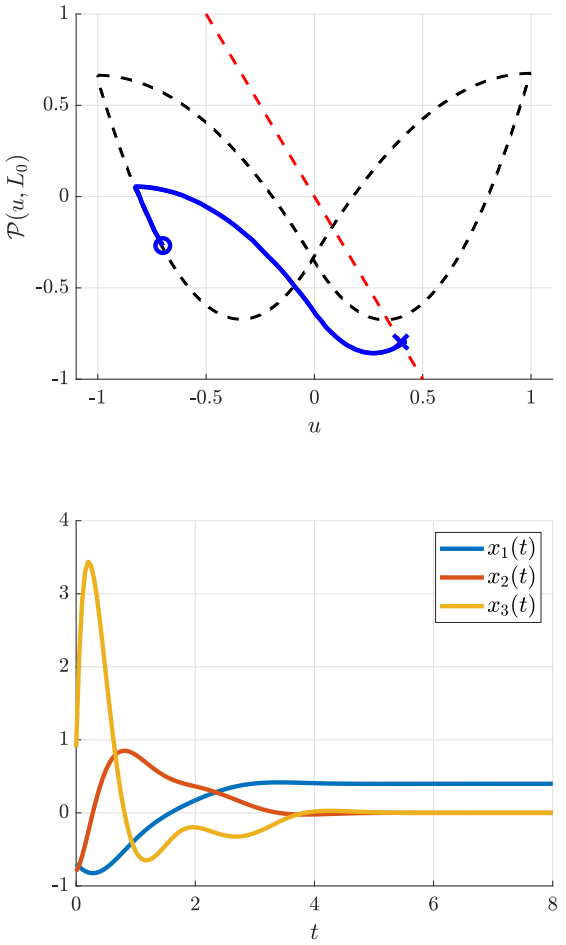

Figure 4.4: Results of a simulation of a Lur'e system whose nonlinearity is the Preisach butterfly operator with a weighting function defined as in (3.4). (a) Input-output phase plot. The black dashed line shows the major hysteresis loop, the red dashed line is a linear line with the slope of $\frac{1}{CA^{-1}B} = -2$ that indicates the input-output pairs which correspond to states $(\bar{x}, \bar{L}) \in \mathscr{E}$, and the simulation is indicated by the blue line where the initial input-output $(u(0), y(0))$ is indicated by the circle and the final input-output $(u(t_f), y(t_f))$ is marked by the cross. (b) Linear system states.

Let the Preisach multi-loop operator $\mathscr{P}$ in this Lur'e system have the weighting function defined by (3.21) in the example of Subsection 3.2.2. It can be checked that $\lambda_M = \frac{4}{\pi}$ and $\lambda_m = -\frac{1}{2\pi}$. Moreover, it can be checked that conditions of Proposition 4.3 are satisfied and consequently this feedback interconnection is stable. The results of a simulation of this Lur'e system with initial conditions of the linear system given by $x_0 = [0.8, -1.0, -1.0]^\top$ and initial interface for the Preisach multi-loop operator given by $L_0 = \{(\alpha,\beta) \in P \mid 0 < \alpha < 1, \beta = -0.9\} \cup \{(\alpha,\beta) \in P \mid \alpha = 1, \beta < -0.9\} \cup \{(\alpha,\beta) \in P \mid \alpha = 0, -0.9 < \beta\}$ is illustrated in Fig. 4.5.

4.3 Conclusions

In this chapter, we studied the absolute stability property of a linear system with a Preisach butterfly and multi-loop hysteresis operators in the feedback loop. Using a differential formulation of the Preisach hysteresis operator, we provided sufficient conditions that guarantee the stability of the closed-loop with respect to a set of equilibria and show the property of its asymptotic behavior.

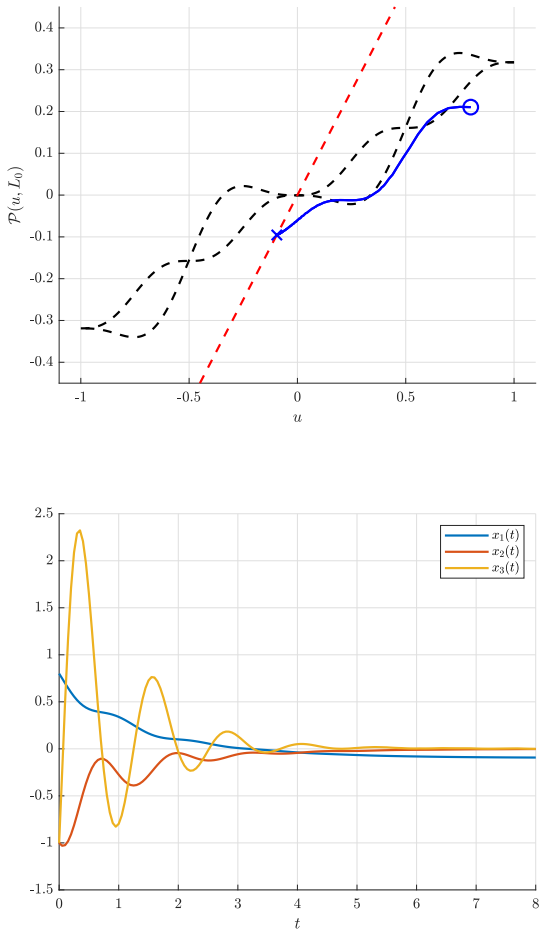

Figure 4.5: Results of a simulation of a Lur'e system whose nonlinearity is the Preisach multi-loop operator with a weighting function defined as in (3.21). (a) Input-output phase plot. The black dashed line shows the major hysteresis loop, the red dashed line indicates the input-output pairs which correspond to states $(\bar{x}, \bar{L}) \in \mathscr{E}$, and the simulation is indicated by the blue line where the initial input-output $(u(0), y(0))$ is indicated by the circle and the final input-output $(u(t_f), y(t_f))$ is marked by the cross. (b) Linear system states.